Hindawi
International Journal of Aerospace Engineering
Volume 2023, Article ID 9991100, 11 pages
https://doi.org/10.1155/2023/9991100

*Research Article*

# Robust Adaptive Beamformer Based on Constant Modulus Penalty Criteria

**Chuanhui Hao,[1] Bin Zhang,[2] and Xubao Sun[1]**

[1]*College of Electrical Engineering and Automation, Shandong University of Science and Technology, Qian Wan Gang Road, No. 579 266590 Qingdao, China*
[2]*College of Computer and Information Engineering, Dezhou University, No. 566 University Rd. West, Decheng District, Dezhou, China*

Correspondence should be addressed to Xubao Sun; hchh518666@sina.com

Received 17 December 2022; Revised 11 July 2023; Accepted 5 September 2023; Published 4 October 2023

Academic Editor: Tuo Han



In this study, a robust adaptive beamformer based on constant modulus (CM) criteria is developed to improve the robustness of the array beamforming, which is a reconstructing minimal optimization for solving the mismatch problem of weight vector caused by steering vector mismatch. In the global positioning system (GPS) L1 band, firstly, a GPS array signal is modelled by designing a dual-polarized antenna array. Secondly, the distortion problem of beamforming is formulated in the traditional minimum variance distortionless response (MVDR) beamformer. For repairing the weight vector mismatch problem, a novel beamformer based on the CM envelope response is proposed to reconstruct MVDR beamforming in the array processing. Besides, min-max penalty criteria are used to enable the beamformer to allocate more degrees of freedom (DOFs) when penalizing the MVDR beamformer responses. Finally, an auxiliary two-element real variable is designed to plan the proposed beamformer. But it is still a nonconvex quadratic programming problem, so an alternating direction method of multipliers (ADMM) is employed to transform the objective function into several subproblems. Illustrative numerical simulation results are provided for validating the effectiveness of the proposed beamformer by comparing it with other existing approaches.

## 1. Introduction

With the development of a robust adaptive beamformer (RAB), the concerns over its reliability also heighten in the global positioning system (GPS). But, because of multiple interferences (i.e., jamming signals, calibration errors, and distorted antenna shape), the antijamming robustness of RAB severely degrades in real applications, wherein the mismatching error between the presumed and actual response is the most commonly affected by the interferences [1]. To solve this problem, a special case of null-steering technique-based dual-polarized array response is proposed to provide double degrees of freedom (DOFs) [2, 3]. Here, it cannot only help the beamformer obtain the desired signal from the mismatch polarization [2] but also prove the more 2 N-1 DOFs in comparison with the N-element single-polarized array.

Beyond that, some diagonal loading (DL) techniques with various uncertainty sets of the steering vector (SV) are studied to obtain a good antijamming RAB. Such as in [4], the sample covariance matrix of RAB is regularized by using a symmetric tridiagonal loading factor. Undeniably, a suitable factor of the projection subspace is difficult to achieve, affecting the robustness of antijamming beamforming. Then, a time-variant factor via the uncertain set constraints is proposed in the paper [5]. However, it is still faced with a crucial problem with the selection of the loading level. Then, a fixed DL factor-based eigenvalue is selected to enhance the antijamming robustness of array processing in [6]; however, this approach must be built on a fixing transformation of the covariance matrix. In [7], a DL beamformer based on the sample matrix inversion is presented to adaptively steer the beamforming, but it is still sensitive to the accuracy of the sample covariance matrix of the array response. Additionally, in [8], adaptive beamforming is obtained by using the DL technique, which is able to steer the beamforming at a small number of samples.

Unfortunately, this DL beamforming is subject to the limitations of the small sampling snapshots so that exists a mismatch error between the likelihood estimation and the reality in the signal processing response. In particular, if the desired signal is contained in the small sampling snapshots, the imprecise SV estimation of these DL beamforming severely degrades the antijamming robustness.

In another class of RAB techniques, eigenspace-based approaches are exploited to construct the subspace of the input signal. For example, in [9], the antijamming weight vector of the subaperture is obtained to generate some nulls from the jamming direction in the eigenspace-based beamformer; however, some prior conditions must be known when the array beamforming is achieved, otherwise not. In [10], the sampling covariance matrix is reconstructed to obtain the antijamming RAB by using the orthogonality between the SV subspace and the interference subspace, but there still exists a calibration error in steering beamforming. Then, an eigenspace-based beamformer is reconstructed by solving the linear problem of SV subspace projection in the array response, i.e., the Capon spatial spectrum in [11]. But this eigenspace is still sensitive to the sample snapshots and the input signal-to-noise ratio (SNR). Additionally, there are some antijamming beamformers that combat the small snapshots, enhancing the robustness of beamforming. For example, in [12], a Lagrange multiplier based on loading sample matrix inversion (LSMI) is used to obtain the RAB in each iteration. But due to the array calibration error, the novanishing SV error still severely degrades the robustness of beamforming. In another example from [13, 14], there are two different beamformers being designed by using the modified NCCB (norm-constrained Capon beamformer) approach and the WC (worst case) method, but the computational time can cost higher than that of LSMI for the same number of antennas. In [15], an antijamming problem of RAB is solved by using the spatial filtering techniques in the radar beamforming, but the precision of beamforming also suffers from the SV error in the iteration; meanwhile, the computational cost of that RAB is higher than the smaller interval needed. Then, a RAB based on minimum variance distortionless response (MVDR) is considered by solving the output power maximization problem and SV mismatch error in [16]. Although the MVDR beamformer can obtain the signal-of-interest steering vector through a double-sided norm perturbation constraint and a similarity quadratic constraint, it is still a quadratically constrained quadratic programming (QCQP) problem with inhomogeneous constraints. When facing the QCQP problem of RAB, the mismatch error of the array response can seriously reduce the robustness of the beamformer. For solving the mentioned QCQP problem, this paper employs a variable splitting technique such as the alternating direction method of multipliers (ADMM), where the ADMM technique is an efficient dual-decomposed optimisation approach that combines the dual-ascent method and the convergence bounded multiplier method. In particular, the dual-ascent performance by adding the convex penalty terms can bring numerical robustness [17].

In this paper, a novel RAB based on the constant modulus (CM) penalty criterion is developed to reconstruct the traditional MVDR beamformer [16]. By contrast, due to CM equalization with constant envelope features, this paper presents the advantage of higher accuracy than the MVDR beamformer [16] under the optimizing weight of RAB per iteration. And the proposed method is computationally superior to the state-of-the-art QCQP problem by using the ADMM variable splitting technique; this is because ADMM has the characteristic of simple update rules and stable-fast convergence to solve the corresponding control variables at each iteration. In addition, our method highlights, compared with the beamformer [16], the following points:

(a) The sample covariance subspace is reconstructed by using the envelope response of the CM array processing in the collected snapshots. This allows the beamformer to enhance the robust adaptation of weight from the spatial blind beamforming

(b) A min-max penalized optimization criterion can manage the CM spatial responses from the sampling interference subspace, which can minimize the maximal penalty term to allocate more DOFs to suppress the interference as well as improve the robust adaptation of the potential SV mismatch constraints in blind beamforming

(c) By designing two auxiliary real-valued conditions, the objective function is converted to solve the rank uncertainty problem, followed by the CVX tool. Then, the beamformer can obtain better robustness than other approaches at a low cost

This paper is organized as follows. In Section 2, a GPS signal is modelled by using a dual-polarized GPS antenna array. In Section 3, the antijamming distortion problem is formulated from a traditional MVDR beamforming. Next, a novel RAB based on the constant modulus (CM) penalty criterion is proposed in Section 4. Finally, the numerical simulations and conclusions are drawn in Section 5 and Section 6, respectively.

*Notation 1.* Table 1 lists this article's operators.

## 2. GPS Signal Model

This paper considers a uniform square antenna array (USAA), as shown in Figure 1, where $2 \times 2$ dual-polarized GPS antenna elements are designed on a dual-layer substrate of "Rogers RO3010 (tm)" substrate with a relative permittivity of 10.2 and a dielectric loss tangent of 0.0035, and the distance between antenna elements is half $\lambda$-wavelength (i.e., about $\lambda = 240\,\text{mm}$ in the GPS L1 band). In USAA, the 8-ports are matched by a 50 Ohm impedance, and then the radiation gains are motivated to obtain the desired GPS signal $\widehat{\mathbf{S}}_x(t)$ by orthogonal linear polarization, where $\widehat{\mathbf{S}}_x(t)$ is an $8 \times 1$ column vector at the time instant as follows:

$$\widehat{\mathbf{S}}_x(t) = \frac{E_0}{\sqrt{2}} \left[ \left( \mathbf{G}_{1,H\theta} - j\mathbf{G}_{1,H\phi} \right), \left( \mathbf{G}_{1,\bar{V}\theta} - j\mathbf{G}_{1,V\phi} \right), \cdots, \left( \mathbf{G}_{4,V\theta} - j\mathbf{G}_{4,V\phi} \right) \right]^T, \tag{1}$$

Table 1: List of operators.

| Symbol | Description |
|---|---|
| Bold letter | Complex matrix |
| $\mathbb{C}$ | Complex space |
| $(\cdot)^H$ | Hermitian transpose |
| $(\cdot)^T$ | Transpose |
| $N(\cdot, \cdot)$ | Gaussian distribution |
| $U(\cdot, \cdot)$ | Uniform distribution |
| $\lvert\cdot\rvert$ | Determinant of a square |
| $\lVert\cdot\rVert^2$ | Euclidean norm |
| $\mathfrak{R}$ | Real parts of complex matrix |
| $\mathfrak{I}$ | Imaginary parts of complex matrix |
| $\sigma^2$ | Received noise power |

where $E_0$ is the amplitude of the minimum guaranteed signal power from the GPS receiver, the subscripts $H$ and $V$ stand for the horizontal and vertical polarization (HP and VP), respectively, and $\mathbf{G}_{i,\mathrm{H/V}}$ is the maximum gain of HP or VP of the $i$ -th antenna element. The jamming signal $\widehat{\mathbf{S}}_j$ has a similar form to the desired signal $\widehat{\mathbf{S}}_x$, which is only considered as deception jamming. Then, in this paper, the GPS transmission signal $\widehat{\mathbf{S}}(t)$ is designed in the GPS L1 band, which is a composite model including a desired GPS signal $\widehat{\mathbf{S}}_x(t)$, jamming signal $\widehat{\mathbf{S}}_j(t)$, and noise $\mathbf{e}(t)$, and all given signals are uncorrelated, as explained in the following equation:

$$\widehat{\mathbf{S}}(t) = \mathbf{\Gamma}(x)\mathbf{a}(\theta_x, \varphi_x)\widehat{\mathbf{S}}_x(t) + \mathbf{\Gamma}(j)\mathbf{a}\left(\theta_j, \varphi_j\right)\widehat{\mathbf{S}}_j(t) + \mathbf{e}(t), \quad (2)$$

where $\mathbf{a}(\theta_x, \varphi_x)$ and $\mathbf{a}(\theta_j, \varphi_j)$ denote the SV at the azimuth-pitch angle ($\theta_x$, $\varphi_x$) and ($\theta_j$, $\varphi_j$) direction, $\mathbf{e}(t)$ obeying to $N(0, \sigma^2)$ as a Gaussian noise is used in $\widehat{\mathbf{S}}(t)$, the symbol $\boldsymbol{\Gamma}$ is defined as an $8 \times 8$ manifold error matrix to repair the desired signal "$x$" and jamming signal "$j$", as follows:

$$\mathbf{\Gamma} \cong \mathrm{diag}\left(\left[1, \eta_1 e^{-j\alpha 1}, \cdots, \eta_{N-1} e^{-j\alpha(i-1)}\right]^T\right), \quad (3)$$

where $\eta_i$ represents the $i$-th gain of USAA, $\alpha_{\mathrm{i}} = (\mathrm{i} - 1)\ \sin\ (\theta)\ \cos\ (\phi)$ is the $i$-th phase shift error corresponding to the $i$-th independent random variables, i.e., the $i$-th steering element $\Gamma_{\mathrm{xi}}(\mathrm{i} = 1, \cdots, 8)$ as the desired $x$-signal.

Then, the corresponding expressions are shown as follows:

$$\Gamma_{xi} = \eta_i e^{-\mathrm{j}\alpha_{xi}} = \eta_i e^{-j(i-1)\ \sin\ (\theta_x)\ \cos\ (\varphi_{\mathrm{x}})}, \quad (4)$$

$$\mathbf{a}(\theta, \varphi) = \left[1, \mathrm{e}^{-\mathrm{j}2\pi \mathrm{r}\ \sin\ (\theta)\ \cos\ (\varphi)}, \cdots, \mathrm{e}^{-\mathrm{j}2\pi(\mathrm{i}-1)\mathrm{r}\ \sin\ (\theta)\ \cos\ (\varphi)}\right], \quad (5)$$

where $r$ is the relative ratio between the element distance and the wavelength and $(\theta, \varphi)$ is a pair of the azimuth angle and pitch angle. Let $\widehat{\mathbf{a}}(\theta, \varphi) = \boldsymbol{\Gamma} \cdot \mathbf{a}(\theta, \varphi)$ represent the total SV with array error. Note that RAB is implemented in the expected environment, removing pseudorandom code and carrier error. Namely, the uncorrelated characteristics of a GPS signal are assumed in the stage after despreading and before carrier synchronization.

## 3. Problem Formulation

In traditional MVDR beamformer [16], the directions of arrival (DOAs) of transmission signal and SV are usually known in advance. And let $\mathbf{w}_t = [w_1, w_2, \cdots, w_N]^T \in \mathbb{C}^{N \times 1}$ as the complex weight variable of beamforming, then the output signal from $L$ snapshots is as follows:

$$\boldsymbol{y}(t) = \mathbf{w}_t^H \widehat{\mathbf{S}}(\mathrm{t}). \quad (6)$$

Thus, the output energy is

$$\begin{aligned}\mathbf{P}(\boldsymbol{w}) &= \frac{1}{L}\sum_{t=1}^{L} |\boldsymbol{y}(\mathrm{t})|^2 = \frac{1}{L}\sum_{t=1}^{L} \left|\mathbf{w}_t^H \widehat{\mathbf{S}}(\mathrm{t})\right|^2 \\ &= \mathbf{\Gamma}(\mathrm{x})\left|\mathbf{w}_t^H \mathbf{a}(\theta_x, \varphi_x)\right|^2 \frac{1}{L}\sum_{\mathrm{t}=1}^{L} \left|\widehat{\mathbf{S}}_x(\mathrm{t})\right|^2 \\ &\quad + \mathbf{\Gamma}(\mathrm{j})\left|\mathbf{w}_{\mathrm{t}}^{\mathrm{H}} \mathbf{a}\left(\theta_j, \varphi_j\right)\right|^2 \frac{1}{L}\sum_{t=1}^{L} \left|\widehat{\mathbf{S}}_j(t)\right|^2 + |\mathbf{w}_t|^2 \frac{1}{L}\sum_{t=1}^{L} |\mathbf{e}(t)|^2.\end{aligned} \quad (7)$$

When $L \longrightarrow \infty$, $\mathbf{P}(\boldsymbol{w})$ is rewritten as

$$\mathbf{P}(\boldsymbol{w}) = E\left[|\boldsymbol{y}(t)|^2\right] = \mathbf{w}_t^H E\left[\widehat{\mathbf{S}}(t)\widehat{\mathbf{S}}^H(t)\right]\mathbf{w}_t = \mathbf{w}_t^H \mathbf{R}\mathbf{w}_t, \quad (8)$$

where $\mathbf{R} = E[\widehat{\mathbf{S}}(t)\widehat{\mathbf{S}}^H(t)]$ is the covariance vector of the array response. This beamformer based on the MVDR criterion has the minimum output energy, while the target directional gain keep unchanged, i.e., $\mathbf{w}_t^H \tilde{\mathbf{a}}(\theta, \varphi) = 1$, then the model of the MVDR beamformer is obtained as follows:

$$\begin{aligned}&\min_{\mathbf{w}_t} \mathbf{w}_t^H \mathbf{R}\mathbf{w}_t, \\ &s.t \quad \mathbf{w}_t^H \tilde{\mathbf{a}}(\theta, \varphi) = 1,\end{aligned} \quad (9)$$

where each variable of $(\mathbf{w}_{\mathrm{t}}, \mathbf{R}, \tilde{\mathbf{a}}, \theta, \varphi)$ is explained as weight vector, covariance matrix, steering vector, and azimuth-pitch angle about the beamforming. By using the Lagrange multiplier method, the cost function of the above problem is produced as follows:

$$L(\mathbf{w}_{\mathrm{t}}, \mu) = \mathbf{w}_t^H \mathbf{R}\mathbf{w}_t + \mu\left(\mathbf{w}_t^H \tilde{\mathbf{a}}(\theta, \varphi) - 1\right). \quad (10)$$

When the partial derivative of $L(\mathbf{w}_t, \mu)$ about $\mathbf{w}_t$ is zero, the final solution to (10) is obtained as follows:

$$\mathbf{w}_t = \mu \mathbf{R}^{-1} \tilde{\mathbf{a}}(\theta, \varphi), \quad (11)$$

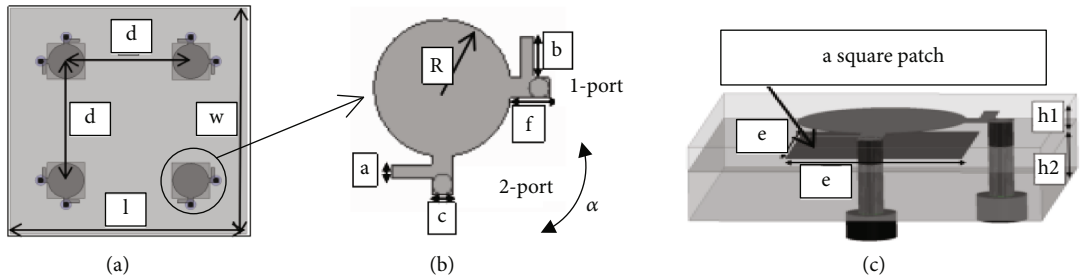


Figure 1: GPS USAA: (a) $2 \times 2$ GPS antenna arrays with $d = 11.6$ cm, $l = w = 2.2$ cm. (b) The upper plane with $R = 16.75$ mm, $a = 3$ mm, $b = 10$ mm, $c = 5$ mm, $f = 9$ mm, $e = 35$ mm, $\alpha = 90\circ$. (c) The side view of antenna cell with $h1 = 5$ mm and $h2 = 10$ mm.

where $\mu = [\tilde{\mathbf{a}}^H(\theta,\varphi)\mathbf{R}^{-1}\tilde{\mathbf{a}}(\theta,\varphi)]^{-1}$. In MVDR beamformer, due to the SV $\tilde{\mathbf{a}}(\theta,\varphi)$ mismatch error including of random error and calibration error [18], the array response can cause weight mismatch problems as follows:

$$\begin{aligned}\mathbf{w}_t &= \mu\mathbf{R}^{-1}\tilde{\mathbf{a}}(\theta,\varphi) = \mu\mathbf{R}^{-1}\boldsymbol{\Gamma}\mathbf{a}(\theta,\varphi)\\ &= \mu\mathbf{R}^{-1}\left[\overline{\boldsymbol{\Gamma}}\left(\overline{\theta},\overline{\varphi}\right) + \overline{\boldsymbol{\Gamma}}(\theta,\varphi) - \overline{\boldsymbol{\Gamma}}\left(\overline{\theta},\overline{\varphi}\right) + \Delta\boldsymbol{\Gamma}(\theta,\varphi)\right]\mathbf{a}(\theta,\varphi)\\ &= \mu\mathbf{R}^{-1}\left(\overline{\mathbf{a}}\left(\overline{\theta},\overline{\varphi}\right) + \underbrace{\overline{\mathbf{a}}(\theta,\varphi) - \overline{\mathbf{a}}\left(\overline{\theta},\overline{\varphi}\right)}_{\text{Random } error} + \underbrace{\Delta\mathbf{a}(\theta,\varphi)}_{\text{Calibration } error}\right)\\ &= \overline{\mathbf{w}}_t + \underbrace{\dot{\overline{\mathbf{w}}}_t - \overline{\mathbf{w}}_t + \Delta\mathbf{w}_t}_{Mismatch}.\end{aligned} \tag{12}$$

Then, in the following section, to reduce the weight mismatch error of beamforming, a novel RAB on based the CM penalty criterion is developed to improve the robustness of beamforming.

## 4. Proposed Method

*4.1. Formulation.* Firstly, for limiting the target SV distortion, a nonlinear inequality relax constraint of $|\mathbf{w}_t^H\tilde{\mathbf{a}}(\theta,\phi)|^2 \le C^2$ is used to repair the constraint condition of the MVDR beamformer. Secondly, a CM envelope response is employed to reconstruct the target output energy of the MVDR beamformer in the collected snapshots. This CM blind channel equalization can obviously improve the robust adaptation of the potential constraints from weight mismatch processing. Finally, a novel optimization problem is formulated as follows:

$$\begin{aligned}&\min_{\mathbf{w}_t}\mathbf{w}_t^H\widehat{\mathbf{R}}\mathbf{w}_t + \left[\left|\mathbf{w}_t^H\widehat{\mathbf{S}}(t)\right|^p - \mu\right]^q\\ &\text{s.t}\begin{cases}\mathbf{w}_t^H\mathbf{w}_t = B\\ \left\|\mathbf{w}_t^H\tilde{\mathbf{a}}(\theta,\varphi)\right\|^2 \le C^2\\ \forall(\theta,\varphi)\in(\Theta,\Phi),\forall t,\end{cases}\end{aligned} \tag{13}$$

where $\Theta$ and $\Phi$ are defined as the discrete angular set of azimuth and pitch direction, the parameter $C \ge 0$ is assumed to be the MVDR constraint supremum, $B$ is a given constant parameter, and $\mu$ is the received signal amplitude of the first snapshot, and the superscript $p - q$ represents the number of constant modulus. In (13), the first constraint $\mathbf{w}_t^H\mathbf{w}_t = B$ states the estimated weight modulus of the allocation variables $\{\mathbf{w}_t^H\mathbf{w}_t\}_{t\in L}$, and the second constraint $|\mathbf{w}_t^H\tilde{\mathbf{a}}(\theta,\varphi)|^2 \le C^2$ represents a nonlinear inequality relaxation to restrict the sidelobe level of beamforming for repairing the SV, i.e., $C = 0.001$ (-30 dB). Next, to consolidate the beamformer, this work is mainly explored from two perspectives:

(1) A min-max recursive criterion-based inequality relaxed constraints is proposed to penalize the spatial responses of interferences as follows

$$\begin{aligned}&\min_{\mathbf{w}_t}\max\{\xi_t\}\\ &\text{s.t}\left\|\mathbf{w}_t^H\tilde{\mathbf{a}}(\theta,\varphi)\right\|^2 \le C^2,\forall(\theta,\varphi)\in(\Theta,\Phi),\forall t,\end{aligned} \tag{14}$$

where the penalty term as $\max\{\xi\}_{t=1}^L$ possesses the minimum output energy as $w_t^H\widehat{R}w_t$ from the MVDR beamformer. Namely, the maximum penalty parameter $\xi$ is regarded as the suppression preference; interferences with the larger $\xi$ have a higher priority to be suppressed. This allows $\max\{\xi\}_{t=1}^L$ to minimize the energy function $w_t^H\widehat{R}w_t$ to obtain the robust response in beamforming. Note that the inequality constraints in (14) are always feasible, and the penalty term can automatically allocate DOFs given by the dual-polarized USAA.

(2) The antijamming weight vector $\mathbf{w}_t$ is obtained by reconstructing the sample covariance subspace of the MVDR beamformer while solving the minimum CM problem of the output beamforming $y(t) = w_t^H\widehat{S}(t)$, as follows

$$\{\mathbf{w}_t\}_{t=1}^L \coloneqq \arg\min_{\mathbf{w}} D(\mathbf{w}_t), \tag{15}$$

where $D(\mathbf{w}_t) = [|\mathbf{w}_t^H\widehat{\mathbf{S}}(t)|^p - \mu]^q$.

By combining (14) and (15), the estimated problem in (13) can be recast to a new object function as follows:

$$\begin{aligned}&\min_{\mathbf{w}_t}\left\{\left[\left|\mathbf{w}_t^H\widehat{\mathbf{S}}(\mathrm{t})\right|^p - \mu\right]^{\mathrm{q}} + \rho\max_t[\xi_t]\right\}\\ &\text{s.t}\begin{cases}\mathbf{w}_t^H\mathbf{w}_t = B\\ \left\|\mathbf{w}_t^H\tilde{\mathbf{a}}(\theta,\varphi)\right\|^2 \le C^2;\forall(\theta,\varphi)\in(\Theta,\Phi),\forall t,\end{cases}\end{aligned} \tag{16}$$

where $\rho \in (0,1)$ is used for the trade-off between antijamming and reducing noise. In practice, the optimization problem in (16) is still nonconvex programming. In general, semidefinite relaxation (SDR) could be used to solve it. But if the rank of the solution is not 1 when SDR is used to eliminate the equation, $\mathbf{w}_t^H \mathbf{w}_t = B$, a nonoptimal solution is possibly obtained [19]. Then, a variable splitting technique based on two-element real-valued conditions is employed to avoid this situation in the following subsection, such as ADMM.

*4.2. Solution Procedure via ADMM.* In this subsection, the ADMM method is used to transform the cost function (12) into several subproblems by variable splitting technique, and for bypassing the difficulty of this work, a penalty parameter $\kappa$ as well as setting $p = 1, q = 2$ are used to rewrite the object functions (16) as follows:

$$\min_{\mathbf{w}_t} \left\{ \left[ \left| \mathbf{w}_t^H \widehat{\mathbf{S}}(t) \right| - \mu \right]^2 + \rho\kappa \right\} \quad \text{s.t} \begin{cases} \mathbf{w}_t^H \mathbf{w}_t = \mathrm{B}, \\ \left\| \mathbf{w}_t^H \tilde{\mathbf{a}}(\theta,\varphi) \right\|^2 \le C^2 \\ \kappa \ge \{\xi\}_{t=1}^L, \forall (\theta,\varphi) \in (\Theta,\Phi), \forall t. \end{cases} \tag{17}$$

Motivated by [20], there are two auxiliary real-valued variables being used as follows:

$$\{\mathbf{m}, \mathbf{n}\} \in \mathbb{C}^{2L\times 1} \mathbf{m} = \mathbf{A}\tilde{\mathbf{w}}, \mathbf{n} = \tilde{\mathbf{w}}, \tag{18}$$

where $\tilde{\mathbf{w}} = \begin{bmatrix} \Re(\mathbf{w}_t) \\ \Im(\mathbf{w}_t) \end{bmatrix}$, $\mathbf{A} = \begin{bmatrix} \Re(\tilde{\mathbf{a}}(\theta,\varphi)) & \Im(\tilde{\mathbf{a}}(\theta,\varphi)) \\ -\Im(\tilde{\mathbf{a}}(\theta,\varphi)) & \Re(\tilde{\mathbf{a}}(\theta,\varphi)) \end{bmatrix}$.

Then

$$\begin{aligned} \tilde{\mathbf{a}}^H(\theta,\varphi)\mathbf{w}_t &= [\Re(\tilde{\mathbf{a}}(\theta,\varphi)) - j\Im(\tilde{\mathbf{a}}(\theta,\varphi))] \\ &\quad \cdot [\Re(\mathbf{w}_t) + j\Im(\mathbf{w}_t)] \left\| \mathbf{w}_t^H \tilde{\mathbf{a}}(\theta,\varphi) \right\|^2 \\ &= \left\| \tilde{\mathbf{a}}^H(\theta,\varphi)\mathbf{w}_t \right\|^2 = \left( \tilde{\mathbf{a}}^H(\theta,\varphi)\mathbf{w}_t \right) \left( \tilde{\mathbf{a}}^H(\theta,\varphi)\mathbf{w}_t \right)^H \\ &= \left( (\Re(\tilde{\mathbf{a}}(\theta,\varphi))\Im(\tilde{\mathbf{a}}(\theta,\varphi)))\tilde{\mathbf{w}}_t \right)^2 \\ &\quad + \left( (-\Im(\tilde{\mathbf{a}}(\theta,\varphi))\Re(\tilde{\mathbf{a}}(\theta,\varphi)))\tilde{\mathbf{w}}_t \right)^2 = \left\| \mathbf{A}\tilde{\mathbf{w}}_t \right\|^2. \end{aligned} \tag{19}$$

Based on the above equations with $\forall (\theta,\varphi) \in (\Theta,\Phi), \forall t$, the multiple constraints with only the real-valued variables can be tackled separately as

$$\min_{\tilde{\mathbf{w}}} \left\{ \left| \left| \tilde{\mathbf{w}}^H \widehat{\mathbf{S}}(t) \right| - \mu \right|^2 + \rho\kappa \right\} \quad \text{s.t} \begin{cases} \mathbf{m} = \mathbf{A}\tilde{\mathbf{w}}\,; \mathbf{n} = \tilde{\mathbf{w}} \\ \|\mathbf{n}\|^2 = B\,; \|\mathbf{m}\|^2 < C^2\,; \kappa \ge \{\xi\}_{t=1}^L, \end{cases} \tag{20}$$

After that, a novel equation based on the augmented Lagrangian method is defined as:

$$\begin{aligned} \ell(\tilde{\mathbf{w}}, \mathbf{m}, \mathbf{n}, \kappa, \boldsymbol{\lambda}_1, \boldsymbol{\lambda}_2) &= \left| \tilde{\mathbf{w}}^H \widehat{\mathbf{S}} - \mu \right|^2 + \rho\kappa + \lambda_1(\mathbf{m} - \mathbf{A}\tilde{\mathbf{w}}) \\ &\quad + \boldsymbol{\lambda}_2(\mathbf{n} - \tilde{\mathbf{w}}) + \frac{\tau}{2}\left( \|\mathbf{m} - \mathbf{A}\tilde{\mathbf{w}}\|^2 + \|\mathbf{n} - \tilde{\mathbf{w}}\|^2 \right) \end{aligned} \tag{21}$$

where $\boldsymbol{\lambda}_1, \boldsymbol{\lambda}_2$ are the Lagrangian multipliers vectors and $\tau > 0$ is the step size. Each computational process is shown as follows:

(1) Solving $\tilde{w}$

By omitting the irrelevant terms, the solution for $\tilde{w}$ in equation (21) is

$$\{\tilde{\mathbf{w}}_{t+1}\} = \arg \min_{\tilde{\mathbf{w}}} \ell\left(\tilde{\mathbf{w}}, \mathbf{m}_t, \mathbf{n}_t, \kappa, \boldsymbol{\lambda}_1^t, \boldsymbol{\lambda}_2^t\right), \tag{22}$$

$$\frac{\partial \ell}{\partial \tilde{\mathbf{w}}} = \mathbf{0} \Rightarrow \tilde{\mathbf{w}}_{t+1} = \frac{1}{2}\mathbf{E}^{-1}\mathbf{F}, \tag{23a}$$

where $\mathbf{E}$ and $\mathbf{F}$ are explained as follows:

$$\begin{aligned} \mathbf{E} &= \widehat{\mathbf{S}}\widehat{\mathbf{S}}^T - \frac{\tau}{2}\left(\mathbf{A}^T\mathbf{A} + \mathbf{I}\right), \\ \mathbf{F} &= 2\mu\widehat{\mathbf{S}}^T + \mathbf{A}^T\left(\lambda_1^t\right)^T + \left(\lambda_2^t\right)^T + \tau\mathbf{A}^T\mathbf{m}_t + \tau\mathbf{n}_t. \end{aligned} \tag{23b}$$

(2) Solving $\mathbf{m}$ and $\mathbf{n}$

Noted where $\mathbf{m}$ is independent with $\mathbf{n}$. For $\boldsymbol{\lambda}_1 = \boldsymbol{\lambda}_1^t$ and $\boldsymbol{\lambda}_2 = \boldsymbol{\lambda}_2^t$, then (21) can be reformulated to two subproblems:

$$\begin{aligned} &\min_{\mathbf{m}} \frac{\tau}{2}\|\mathbf{m} - \mathbf{m}_t\|^2 \\ &\text{s.t} \|\mathbf{m}_t\|^2 \le C^2, \\ &\min_{\mathbf{m}} \frac{\tau}{2}\|\mathbf{n} - \mathbf{n}_t\|^2 \\ &\text{s.t} \|\mathbf{n}_t\|^2 = B, \end{aligned} \tag{23c}$$

where $\mathbf{m}_t = \mathbf{A}\tilde{\mathbf{w}} - \boldsymbol{\lambda}_1^t/\tau$ and $\mathbf{n}_t = \tilde{\mathbf{w}} - \boldsymbol{\lambda}_2^t/\tau$.

Solutions of (23c) are

$$\mathbf{m}_{t+1} = \begin{cases} \dfrac{\mathrm{C}}{\|\mathbf{m}_t\|}\mathbf{m}_t, & \|\mathbf{m}_t\| > C, \\ \mathbf{m}_t, & \|\mathbf{m}_t\| = C, \end{cases} \qquad \mathbf{n}_{t+1} = \frac{\sqrt{\mathrm{B}}}{\|\mathbf{n}_t\|}\mathbf{n}_t, \tag{23d}$$

(3) Maximum penalty parameter $\kappa$

The Karush-Kuhn-Tucker conditions [21] of primal feasibility is the necessary condition to minimize a feasible

**Initialize** $\{\tilde{\mathbf{w}}^0\}$, $\{\mathbf{m}^0\}$, $\{\mathbf{n}^0\}$, $\{\boldsymbol{\lambda}_1^0\}$, $\{\boldsymbol{\lambda}_2^0\}$;
Compute $\hat{\mathbf{S}}$ using ((1)-(2)); Determine $\tilde{\mathbf{a}}(\theta,\varphi)$ using (5);
**Repeat for** t=1,…,L;
Obtain $\mathbf{m}(t+1)$ and $\mathbf{n}(t+1)$ using (23d);
Determine $\kappa$ by solving (23f) using Bisection method;
Obtain $\tilde{\mathbf{w}}(t+1)$ using (23a);
Update $\boldsymbol{\lambda}_1^{t+1}, \boldsymbol{\lambda}_2^{t+1}$ using (23g) and (23h).
**Until end for** t=L;
Output $\tilde{\mathbf{w}} = \begin{bmatrix} \Re(\tilde{\mathbf{w}}^{(t+1)}) \\ \Im(\tilde{\mathbf{w}}^{(t+1)}) \end{bmatrix}$
Final anti-jamming weight $\mathbf{w}_{\text{final}} = \boldsymbol{R}_{j+e}^{-1}\tilde{\mathbf{a}}/\tilde{\mathbf{a}}^{\text{H}}\boldsymbol{R}_{j+e}^{-1}\tilde{\mathbf{a}}/\|\tilde{\mathbf{w}}\|$

Algorithm 1: Blind adaptive antijamming beamforming.

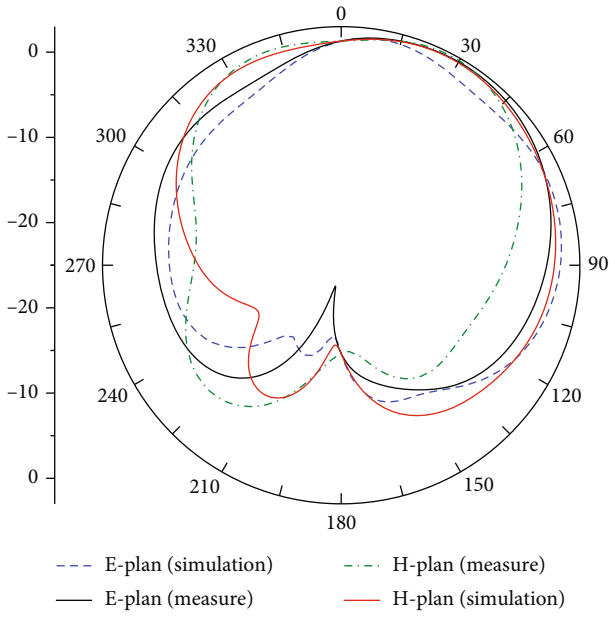


Figure 2: Simulated/measured patterns at the E/H-plane.

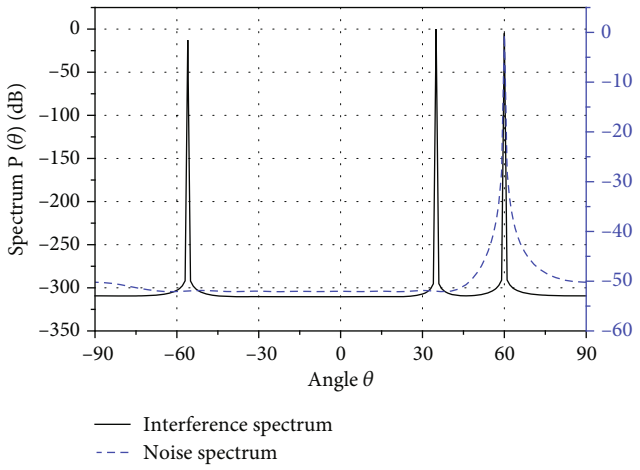


Figure 3: DOA estimation based on the MUSIC algorithm.

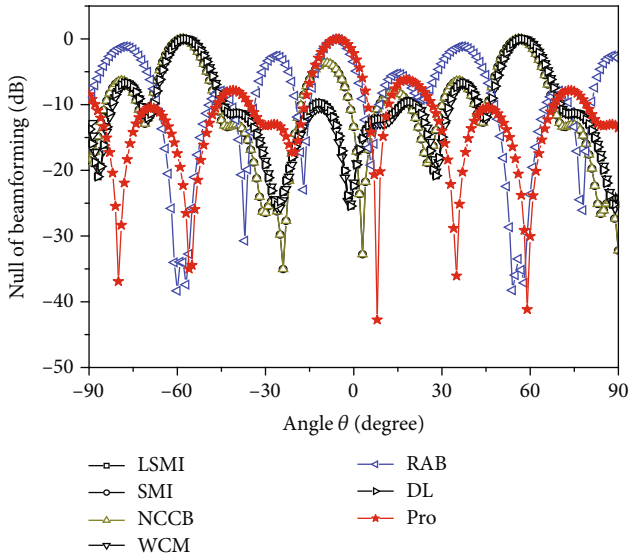


Figure 4: Antijamming beamforming comparison.

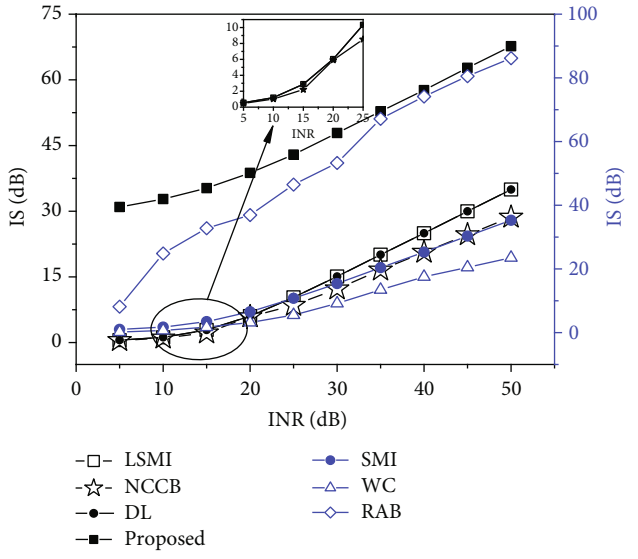


Figure 5: Interference suppression level.

Table 2: Example sets list.

| Scenario | Example error | Vector | Distribution |
|---|---|---|---|
| 1 | Random look direction | DOA | $U(-5\circ, 5\circ)$ |
| 2 | Perturbations | Gain | $N(1, 0.1^2)$ |
| | | Phase | $U(-5\circ, 5\circ)$ |
| 3 | Position error | Space | $U(-\lambda/25, \lambda/25)$ |
| 4 | Coherent local scattering | Manifold error | $U(0, 2\pi)$ |

point of constrained nonlinear programming. Thus, equation (21) with respect to $\kappa$ is equivalent as follows:

$$\begin{aligned} &\min\ \rho\kappa + \boldsymbol{\lambda}_1^t\left[\left(\tilde{\mathbf{w}}^t\right)^H\widehat{\mathbf{S}}(t) - \mu\right] + \frac{\tau}{2}\left\|\left(\tilde{\mathbf{w}}^t\right)^H\widehat{\mathbf{S}}(t) - \mu\right\|^2 \\ &\text{s.t}\quad \kappa \geq \{\xi_t\}_{t=1}^L, \end{aligned} \tag{23e}$$

A Bisection method (The bisection method is a successive nonlinear approximation method that keeps cut the interval $[a..b]$ (sign of $f(a) \neq$ sign of $f(b)$) into 2 halves and check which half interval contains a root of the nonlinear function $f(x)$.) [22] is employed to find the root with respect to $\kappa$ in (23e). That result is shown as:

$$\max\left\{0, \frac{\left|\lambda_1 + \tau\tilde{\mathbf{w}}^H\widehat{\mathbf{S}}(t)\right|}{2\sqrt{\kappa/\xi_t}}\right\} = \rho, \tag{23f}$$

where $\kappa = \max\left(\{\xi_t\}_{t=1}^L \cdot |\Delta|^2\right), \Delta \approx (\boldsymbol{\lambda}_1^t + \tau\tilde{\mathbf{w}}_t^H\widehat{\mathbf{S}})$.

(4) Updating the Lagrangian multipliers $\lambda_1$, $\lambda_2$

$$\lambda_1^{t+1} = \lambda_1^t + \tau\left(m^{t+1} - A\tilde{w}^{t+1}\right), \tag{23g}$$

$$\lambda_2^{t+1} = \lambda_2^t + \tau\left(n^{t+1} - \tilde{w}^{t+1}\right). \tag{23h}$$

Finally, the proposed RAB based on the CM penalty criterion is summarized in Algorithm 1. Here, the computational burden is to find the root in (23f), but the finding root needs to run only once by using the bisection method. And the running time of the designed beamformer mainly depends on the iterative process of solving the weight vector, where the computational complexity is $O(M^3)$ at each iteration.

## 5. Simulation Results

*5.1. The Signal Model Based GPS Antenna Array.* In Ansoft HFSS software, a four-element dual-polarized USAA with $M = 8$ ports is designed to obtain the radiation gains of the antenna array at the GPS L1 band, which can model the GPS signal $\widehat{\mathbf{S}}(t)$. In this work, the results are shown in Figure 2, which shows the normalized gain of the E/H-plane at 1.57 GHz when the first port is active and other ports are terminated in match loads. It is clearly found that the E-plane gain pattern is more symmetrical and has similar "apple-shape" radiation than the H-plane. Although the measured results are lower than the simulation due to the scattering structure errors in the testing environment, the maximal radiation efficiency is almost up to 77.26%. Then, we employ the maximal gains of the E/H-plane to obtain the signal $\widehat{\mathbf{S}}_x$. In addition, the deception jamming $\widehat{\mathbf{S}}_j$ has a similar form with $\widehat{\mathbf{S}}_x$ except for a different power, and the noise $\mathbf{e}(t)$ adopts a Gaussian noise. In short, the performance of dual-polarized USAA meets the requirement of a GPS antenna terminal, and the results are used to receive a GPS signal model $\widehat{\mathbf{S}}(t)$.

*5.2. Antijamming RAB Performance Comparison.* To show the antijamming robustness of that novel beamforming, we list some exciting methods as the references, where there are the optimal beamforming, DL [6], LSMI [12], NCCB [13], WC [14], MVDR [16], and sample matrix inversion-based reconstruction (SMI) [23]. The interference-to-noise ratio (INR) is equal to -15 dB, and the noise obeys a Gaussian distribution $N(0, 1^2)$. The snapshot is set to be $L = 128$, and the computational results are averaged by 200 Monte Carlo trials. The input SNR is set from -20 dB to 20 dB, and the simulation is running with the iteration from 10 to 100.

Firstly, the estimated directions of input signals are obtained as the a priori condition of the simulation experiment. MUSIC (multiple signal classification) [24], where the signal source both interferences and noise are shown in Figure 3. Here, it especially explains that the spectrum data are obtained by the covariance of different signals. In Figure 3, a solid line indicates the spectrum of interference from three peaks at $\theta = (-55\circ, 35\circ, 60\circ)$. While the spectrum peak $P(\theta = 600)$ coincides with the peak of noise, then the DOAs $\theta = (-55\circ, 35\circ, 60\circ)$ are chosen as the directions of interferences. Then, the obtained DOAs and maximum radiation gains from HP and VP are introduced into formula (2) to generate the signal model.

Next step, the antijamming comparisons of beamforming based on the a priori DOAs condition are shown in Figure 4. Here, the SNR = 20 dB and INR = 10 dB are chosen as other a priori conditions in the simulation experiment. It is clearly found that all valley points can be well located in the DOAs from the spectrum peaks shown in Figure 4. Note that the number of interference sources is $2\,\mathrm{N} - 1 = 7$ while there are three interference sources [i.e., DOAs = $(-55\circ, 35\circ, 60\circ)$] in Figure 4; this is because the azimuth angle is only chosen as the half number

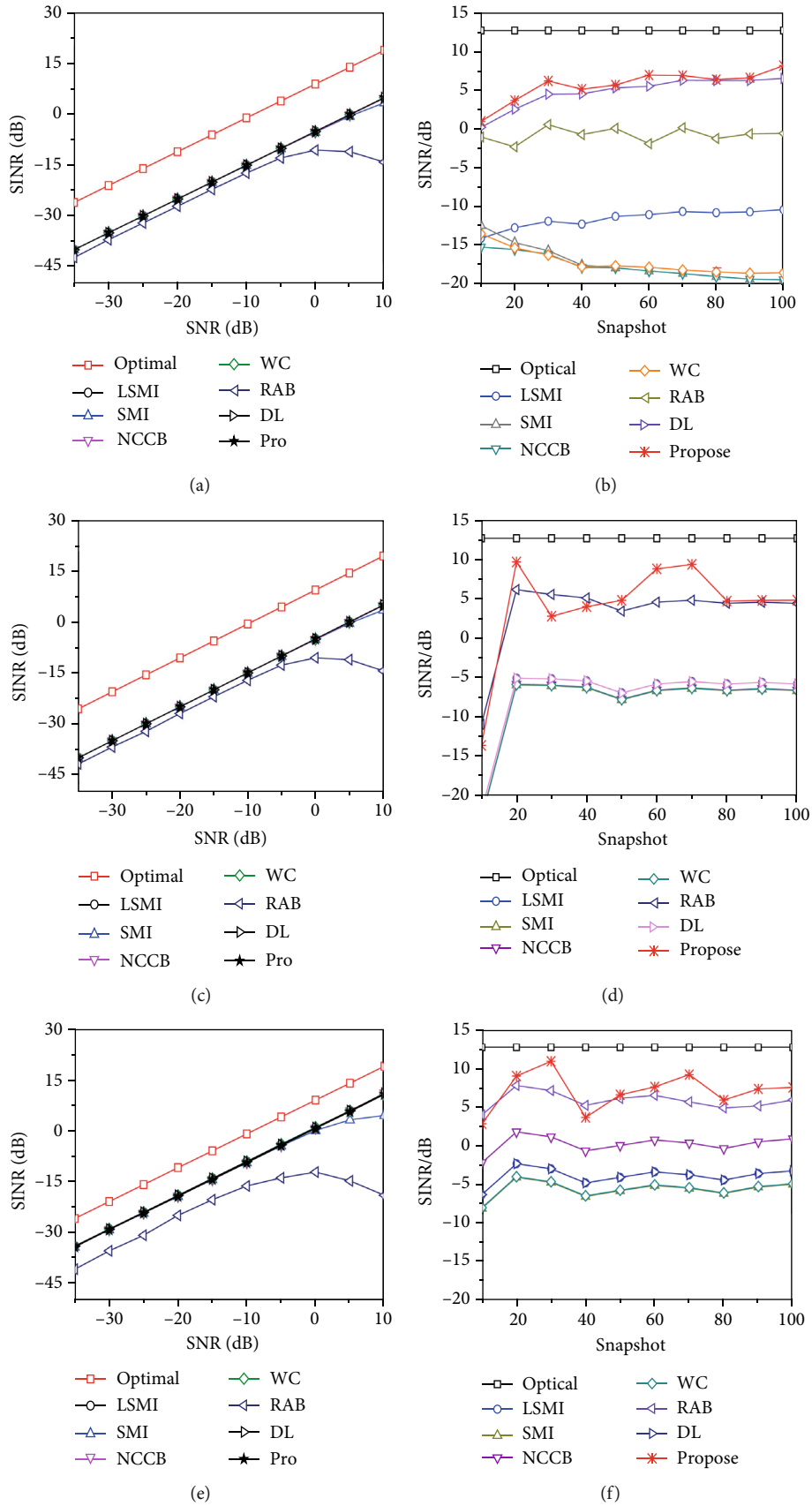


Figure 6: Continued.

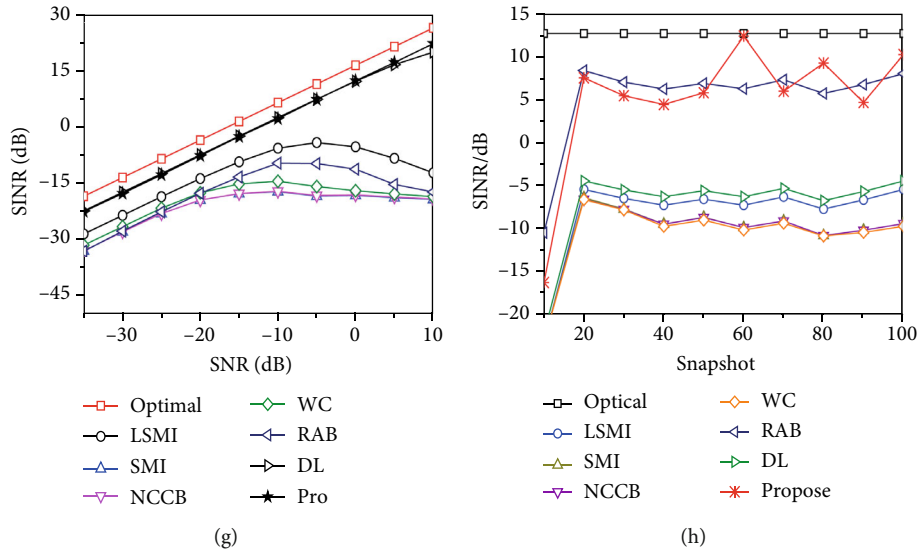


Figure 6: Example sets from scenario 1 to 4: (a), (c), (e), and (g) versus input SNR: (b), (d), (f), and (h) versus number of snapshots.

of the whole angle from -180° to 180°. By comparing the proposed method with LSMI and RAB, it can be observed that the antijamming null attenuates stronger than 38 dB in the jamming direction and the beamforming has a lower side lobe in all nonjamming directions. The conclusion of this experiment is that the proposed approach has good robustness to antenna array perturbation due to its constant modulus smooth characteristic in the beamforming.

Besides, for showing the comparison of beamforming power, the interference suppression (IS) levels are used as an important index of before and after antijamming work. Figure 5 plots IS levels by using the existing beamformers, where the black and blue graphs are pointed to the left black label and the right blue label, respectively. It can be found that the proposed method obtains the best antijamming level from $INR = 5$ dB to 35 dB in all approaches. This is because the penalty variable max $\{\xi\}_{t=1}^{L}$ can automatically enable the reconstructed beamformer to distribute more DOFs to suppress interferences in the spatial signal responses. Although its IS level is slightly worse than RAB, from 35 dB to 50 dB, the IS level gradually enhances along with the INR increase.

Finally, we list four scenarios as presented in Table 2, where the different example errors are shown to explore the robustness of antijamming beamforming by using the signal-to-interference plus noise ratio (SINR) comparison versus snapshots and SNR.

Scenario 1 considers the SINR comparison versus input SNR and the number of snapshots in random look direction errors. As shown in Figure 6(a), all existing beamformers can perform good SINR performance along with SNR increasing, but when SNR exceeds zero dB, RAB shows worse performance due to SINR decline. Additionally in Figure 6(b), we can clearly find that the proposed method performs best among all methods along with the growth of snapshots. This is because the used CM criteria can enable the beamformer to collect the max-stable power from look direction errors when SNR and snapshots gradually increase. But the SINR of LSMI and NCCB degrade along with the snapshots increasing. In scenario 2, we discuss the effects of antijamming beamforming in gain and phase perturbations. In Figure 6(c), along with the input SNR increasing, we can observe that the antijamming performance of all existing beamformers can show good robustness except RAB. In Figure 6(d), due to the gain and phase smooth perturbations, the proposed method performs the best SINR level versus the number of snapshots. Scenario 3 considers that the antenna element error is caused by the position mismatch. Figures 6(e) and 6(f) depict the robustness against antenna position error. We can observe that the SINR level of all beamformers can obtain the enhancement at $-30\,dB < SNR < 0$ dB. Especially in the field of navigation, the proposed method performs best when the SNR is generally -30 dB. And when the number of snapshots exceeds 60, the proposed method outperforms other methods. In scenario 4, the coherent local scattering can cause the SV distortion in (12). The final results are shown in Figures 6(g) and 6(h), where the proposed method provides the best performance among all beamformers when the number of snapshots exceeds 50, while the SINR of NCCB, WC, LSMI, and RAB show a downward trend versus the input SNR increasing.

From the above analysis, it is illustrated that the proposed RAB can obtain good robustness of beamforming in all existing beamformers. However, the SINR of RAM suffers from performance degradation when the input SNR increases in all scenarios. Although the weight vectors of WC and NCCB can be solved by the CVX tool, the objective solution sometimes appears in the local optimization when the nonconvex nonlinear optimization is solved by the long running time. LSMI can give an efficient solution to find the optimal loading level, but an inaccurate loading sample leads to an imprecise Lagrangian multiplier. In contrast, the proposed RAB based on CM envelope response can obtain the robust adaptation of weight vector mismatch constraints in the spatial beamforming; further, the antijamming

robustness of beamforming is also improved by the simple update rules and stable-fast convergence.

## 6. Conclusion

In this paper, we propose a novel beamformer via the constant modulus (CM) penalization criteria to improve the antijamming robustness of beamforming. Wherein, the CM envelope response is used to obtain the robust adaptation of weight vector mismatch by reconstructing the MVDR beamformer in collected snapshots, and a min-max penalized function is proposed to penalize the spatial responses of the array signal model. This can enable the reconstructed beamformer to allocate more DOFs to suppress the interferences. However, a nonconvex quadratic program problem is formulated in this beamformer, and then we use the ADMM optimization method to solve this quadratic problem. According to the SINR, some simulations show that the proposed beamformer can achieve better antijamming robustness in beamforming by competing with the exciting beamformers.

## Data Availability

For example, "Data availability statement: The data that support the findings of this study are available on request from the corresponding author." The (gains of antenna array) data used to support the findings of this study were supplied by (ORCID ID: 0000-0002-9623-8296) under license and so cannot be made freely available. Requests for access to these data should be made to (ORCID ID: 0000-0002-9623-8296).

## Disclosure

This was performed as part of the employment of Xubao Sun because Xubao Sun as a funder was involved in the manuscript writing.

## Conflicts of Interest

The authors declare that they have no conflicts of interest.

## References

[1] G. P. Blasone, F. Colone, P. Lombardo, P. Wojaczek, and D. Cristallini, "Passive radar STAP detection and DoA estimation under antenna calibration errors," *IEEE Transactions on Aerospace and Electronic Systems*, vol. 57, no. 5, pp. 2725–2742, 2021.

[2] M. G. Amin, "Sequential interference nulling and localization in two-dimensional GPS receiver array," in *Proceedings of the 20th International Technical Meeting of the Satellite Division of The Institute of Navigation (ION GNSS 2007)*, pp. 1257–1264, Fort Worth, TX, USA, 2007.

[3] R. L. Fante and J. J. Vaccaro, "Evaluation of adaptive space time polarization cancellation of broadband interference," in *2002 IEEE Position Location and Navigation Symposium (IEEE Cat. No.02CH37284)*, pp. 1–3, Palm Springs, CA, USA, 2002.

[4] M. Zhang, X. Chen, and A. Zhang, "A simple tridiagonal loading method for robust adaptive beamforming," *Signal Processing*, vol. 157, pp. 103–107, 2019.

[5] J. Yang, W. X. Li, Y. Zhang, and J. Lu, "Robust wideband beamforming method for linear frequency modulation signals based on digital dechirp processing," *IET Radar, Sonar & Navigation*, vol. 13, no. 2, pp. 283–289, 2019.

[6] M. S. Hossain, G. N. Milford, M. C. Reed, and L. C. Godara, "Efficient robust broadband antenna Array processor in the presence of look direction errors," *IEEE Transactions on Antennas and Propagation*, vol. 61, no. 2, pp. 718–727, 2013.

[7] C. Ryan and J. R. Buck, "Applying the unit circle constraint to the diagonally loaded minimum variance distortionless response beamformer," in *2017 IEEE International Conference on Acoustics, Speech and Signal Processing (ICASSP)*, pp. 3366–3369, New Orleans, LA, USA, 2017.

[8] Y. Jian, L. Rui-qi, and X. Xu-qi, "A adaptive beamforming design in low sample number conditions based on diagonal loading algorithm," in *2016 IEEE International Conference on Signal and Image Processing (ICSIP)*, pp. 755–758, Beijing, China, 2016.

[9] C. Wang, J. Tang, and Y. Wu, "Eigenspace-based beamforming technique for multipath coherent signals reception," *Signal Processing*, vol. 128, pp. 150–154, 2016.

[10] X. Zhu, X. Xu, and Z. Ye, "Robust adaptive beamforming via subspace for interference covariance matrix reconstruction," *Signal Processing*, vol. 167, no. 12, article 107289, 2020.

[11] Z. Zheng, W. Q. Wang, H. C. So, and Y. Liao, "Robust adaptive beamforming using a novel signal power estimation algorithm," *Digital Signal Processing*, vol. 95, no. 11, article 102574, 2019.

[12] X. X. Li, D. W. Wang, X. Ma, and Z. Xiong, "Robust adaptive beamforming using iterative variable loaded sample matrix inverse," *Electronics Letters*, vol. 54, no. 9, pp. 546–548, 2018.

[13] W. X. Li, X. J. Mao, and W. H. Yu, "Robust adaptive array beamforming based on modified norm constraint algorithm," *Applied Computational Electromagnetics Society Journal*, vol. 29, no. 12, pp. 1060–1066, 2014.

[14] Y. Huang, S. A. Vorobyov, and Z. Luo, "Quadratic matrix inequality approach to robust adaptive beamforming for general-rank signal model," *IEEE Transactions on Signal Processing*, vol. 68, pp. 2244–2255, 2020.

[15] J. H. Qian, Z. He, W. Zhang, Y. Huang, N. Fu, and J. Chambers, "Robust adaptive beamforming for multiple-input multiple-output radar with spatial filtering techniques," *Signal Processing*, vol. 143, pp. 152–160, 2018.

[16] Y. Huang, M. Zhou, and S. A. Vorobyov, "New designs on MVDR robust adaptive beamforming based on optimal steering vector estimation," *IEEE Transactions on Signal Processing*, vol. 67, no. 14, pp. 3624–3638, 2019.

[17] S. Yuyu, W. Tong, and L. Xuefang, "Decoupled narrowband robust adaptive beamforming based on the ADMM in a noisy channel," *IET Radar, Sonar Navigation*, vol. 14, no. 4, pp. 637–642, 2020.

[18] W. Chen, Y. Zhao, and J. Gao, "Improved capon beamforming algorithm by using inverse covariance matrix calculation," in *IET International Radar Conference 2013*, Xi'an, 2013.

[19] A. Khabbazibasmenj, S. A. Vorobyov, and A. Hassanien, "Robust adaptive beamforming based on steering vector estimation with as little as possible prior information," *IEEE Transactions on Signal Processing*, vol. 60, no. 6, pp. 2974–2987, 2012.

[20] J. Liang, H. C. So, J. Li, A. Farina, and D. Zhou, "On optimizations with magnitude constraints on frequency or angular responses," *Signal Processing*, vol. 145, pp. 214–224, 2018.

[21] Y. Ali, Z. Shen, F. Zhu et al., "Solutions verification for cloud-based networked control system using Karush-Kuhn-Tucker conditions," in *2018 Chinese Automation Congress (CAC)*, pp. 1385–1389, Xi'an, China, 2018.

[22] P. Mejzlík, "A bisection method to find all solutions of a system of nonlinear equations," *Providence: AMS*, vol. 277, 1994.

[23] Z. Guan, H. Shi, L. Zhang, and N. Ma, "Low-complexity robust adaptive beamforming based on covariance matrix reconstruction," in *Signal Processing, and Systems. CSPS 2018*, vol. 515 of Lecture Notes in Electrical Engineering, Springer, Singapore.

[24] B. Vikas and D. Vakula, "Performance comparision of MUSIC and ESPRIT algorithms in presence of coherent signals for DoA estimation," in *2017 International Conference of Electronics, Communication and Aerospace Technology*, pp. 403–405, Coimbatore, India, 2017.